Influence of light-ion irradiation on the heavy-ion track etching of polycarbonate

R.S. Thomaz · C.T. de Souza · R.M. Papaléo

Abstract We report on the effect of light-ion irradiation on the size distribution of etched tracks produced by medium energy heavy-ions in polycarbonate. Makrofol KG polycarbonate foils were treated with 2 MeV H^+ ions at different fluences ϕ either before or after a short irradiation with 18 MeV Au^{7+}. The heavy ion irradiation was used to produce the latent tracks in the foils and the proton beam acted as a perturbation to the matrix. The proton irradiation causes initially a decrease in the mean etched pore size, as compared to samples only bombarded by Au ions, reaching a minimum at H^+ fluences around 2–5×10^{13} cm^{-2}, while at higher ϕ the pore size starts to grow again. This effect is attributed to the action of two competitive processes that dominate in different fluence regimes. The decrease in the pore radii at low fluences is attributed to an increase in crystallinity induced by the proton beam. As the total dose builds up, this effect is surpassed by chain scission and amorphization that grow at a lower rate and cause the pore radii to increase again.

Keywords Ion track etching · Polymers · Polycarbonate

1 Introduction

The damaged region created around swift heavy-ion trajectories in dielectric materials often exhibits a different chem-

R.S. Thomaz · C.T. de Souza · R.M. Papaléo (✉)
Faculty of Physics, Catholic University of Rio Grande do Sul,
Av. Ipiranga 6681, 90691-900 Porto Alegre, Brazil
e-mail: papaleo@pucrs.br

Present address:
C.T. de Souza
Graduate Program of Materials Science, Federal University of Rio
Grande do Sul, Av. Bento Gonçalves 9500, Porto Alegre, Brazil

ical reactivity than the unmodified surroundings. Therefore, when the bombarded region is exposed to an appropriate etching agent, the ion tracks can be developed to tailor micro or nanostructures on surfaces or to modify materials properties [1, 2]. Track-etching has been extensively applied in particle detectors [1] and in the processing of membranes with a narrow distribution of pore sizes, especially using polymeric materials [3, 4].

Ion track etching is most commonly investigated using beams of heavy ions at high velocities (∼1 MeV/u or larger) [1–3] available only at a few large irradiation facilities around the world. Recently, the prospects of ion track etching with beams of lower energy (of the order of 0.1 MeV/u), available at standard medium-energy ion implanters [5–8], have also been investigated. In the wake of low-velocity heavy ions, sufficiently high density of excitations is still achievable along penetration depths of less than a couple of microns. Therefore, this energy regime is suitable for the application of ion tracks in the nanostructuring of thin layers or the near surface of thicker materials.

Because of its excellent mechanical properties and high sensitivity to the track etching, polycarbonate (PC) has been extensively investigated [1, 3, 9–12], and is commercially available as precise pore diameter membranes for filtering, detection of contaminants, and other biomedical applications [13]. In this work, we investigated the effect of a 2 MeV H^+ treatment on the etching response of the foils to 18 MeV Au^{7+} ions. Contrary to previous work that observed an increase in the etched track radius for PC bombarded by 62 MeV H^+ and exposed to fission tracks [12], here we observe a more complex behavior, with a sharp decrease in the pore size at low fluences, followed by a slow regrowth of the radii size at the largest fluences. This shows that the proton beam generates two competitive processes: one with large

cross-section that slows down the radial etching rate and another with a small cross-section that tends to accelerate the bulk etching rate.

2 Experimental

The samples were made of polycarbonate (PC) foils (Makrofol KG, Bayer, Germany), about 12 μm thick. Before the experiments, the near surface of the foils was etched away with a 6 M NaOH solution for 10 min. The targets were then exposed, in sequence, to two different ion beams. In one set of samples, the foils were initially pre-treated with 2 MeV H^+ ions with fluences ranging from 5×10^{12} to 5×10^{14} ions/cm² at a current density of ~30 nA/cm², and subsequently bombarded with a 18 MeV Au^{7+} beam at a fluence of ~5×10^8 ions/cm². In another set of samples, the irradiation order was reversed. In both cases, the heavy ion irradiation was used to produce the latent tracks in the foils and the proton beam acted as a perturbation to the PC matrix. The sequence of irradiations was performed at the 3 MV HVEE Tandetron accelerator at the Federal University of Rio Grande do Sul, Porto Alegre, Brazil, at room temperature and with the samples held at a vacuum of ~10^{-6} Torr. The estimated projected ranges R_p in the foils obtained from the SRIM 2010 code [14] are 66.5 μm for the 2 MeV H^+ beam and 6.6 μm for the 18 MeV Au ions. The dE/dx for the proton beam is almost constant through out the foil with a value around 2 eV/Å. The irradiated foils were etched with 6 M NaOH solution in a thermal bath at $60 \pm 1\,°C$ for 1 to 3 minutes with continuous magnetic agitation. A total of 4 batches of samples, irradiated and processed in different days, were analyzed: three with the H + Au and one with Au + H beam sequences. Even with the controlled conditions adopted, the bulk etching rate showed some variability from batch to batch, mainly when a different brand of NaOH was used.

The etched surfaces were analyzed by scanning electron microscopy, using a Philips XL30 microscope and Au coating. Gel permeation chromatography (GPC) was performed using *Styragel* columns and detection by index of refraction. $CHCl_3$ was used as eluant at a flux of 1 mL/min. X-ray diffraction measurements were carried out with a Shimadzu XRD 7000 diffractometer with a graphite monochromator and using $CuK\alpha$ X-rays ($\lambda = 1.5402$ Å). The diffraction patterns were collected in the 2θ range of 5–40° in 0,05° steps with 5 s acquisition per point (scanning speed of 0.6°/min). Contact angle measurements were performed using the sessile drop technique and averaging the results obtained for 5 droplets of water deposited in different regions of the samples.
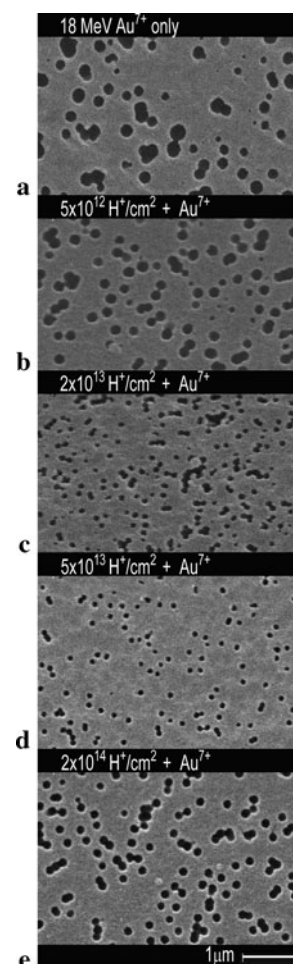

Fig. 1 SEM images of etched ion tracks on PC foils bombarded with 2 MeV H^+ at different fluences. The samples were first bombarded by the H^+ beam and subsequently irradiated with the 18 MeV Au beam to produce the etchable tracks. (**a**) Control sample (Au beam only); (**b**) $\phi = 5 \times 10^{12}$ H^+/cm²; (**c**) $\phi = 2 \times 10^{13}$ H^+/cm²; (**d**) $\phi = 5 \times 10^{13}$ H^+/cm²; (**e**) $\phi = 2 \times 10^{14}$ H^+/cm²

3 Results

The pores generated on PC foils bombarded by 2 MeV H^+ + 18 MeV Au^{7+} and etched in NaOH for 2 min are shown in Fig. 1 for various proton fluences. It is seen that the proton irradiation causes initially a decrease in the etched pore size as compared to samples not treated with the proton beam. The reduction effect is greatest at H^+ fluences around 2 to 5×10^{13} cm⁻². At higher H^+ fluences, the pore size starts to slowly grow again, but in the fluence range investigated, they were still smaller than the control samples (bombarded only with 18 MeV Au). The trend (steep decrease of the hole diameter at low H^+ fluences, followed by a slow recovery of the size at higher fluence) was the same for samples bombarded in the reverse order Au + H (first with 18 MeV Au and subsequently with 2 MeV H^+).

Due to the high sensitivity of the final etched pore diameter to the etching conditions [10], especially at the short etching times employed, the values of the mean pore diameter may vary among batches prepared under similar conditions. For the 3 batches prepared using the irradiation order H + Au (batches 1–3), the mean pore diameter in the control samples (no H^+ irradiation) of batches 1 and 2 were
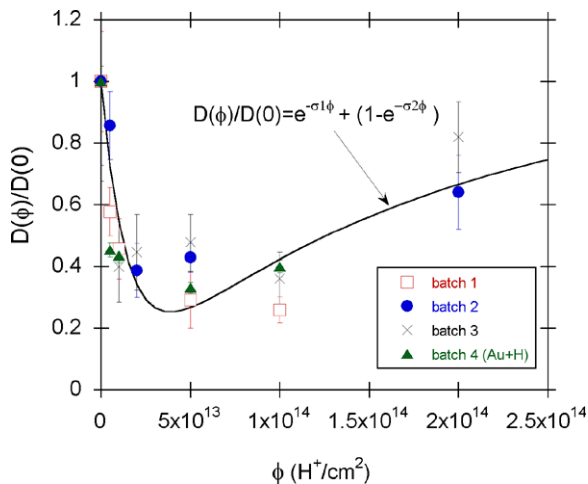
$$\frac{D(\phi)}{D(0)} = e^{-\sigma_1\phi} + (1 - e^{-\sigma_2\phi})$$

Fig. 2 Normalized diameter of the etched pores ($D(\phi)/D(0)$) as a function of H^+ fluence ϕ, for four batches of samples. $D(0)$ is the diameter in the samples bombarded with Au only. The solid line is the best fit of the function $D(\phi)/D(0) = e^{-\sigma_1\phi} + (1 - e^{-\sigma_2\phi})$ to the data points, obtained with $\sigma_1 = 7.2 \times 10^{-14}$ cm^2 and $\sigma_2 = 5.7 \times 10^{-15}$ cm^2

$\sim$20% different (260 nm and 220 nm, respectively). For the batch 3, where a different NaOH was used, presumably of poorer quality, the mean pore size decreased by 50%. Thus, in order to compare the evolution of the pore size with the proton fluence ϕ, the normalized mean pore diameter $D(\phi)/D(0)$ was used, where $D(0)$ is the diameter of the sample with no H^+ irradiation. It is seen in Fig. 2 that all batches (including batch 4, prepared in the reverse irradiation order, Au + H) showed a similar dependence with H^+ fluence ϕ. The pore diameter diminishes down to a minimum value around $0.3D(0)$ and at larger fluences slowly re-growth. The effect of H^+ irradiation could be followed up to $\phi = 2 \times 10^{14}$ H$^+$/cm^2. At $\phi = 5 \times 10^{14}$ H$^+$/cm^2 the proton irradiated PC foils became too brittle and did not withstand the additional increase in mechanical fragility introduced by the pore opening.

The observation of a minimum in the curve of the pore diameter versus fluence is compatible with the existence of two competitive effects induced by the proton beam: one that causes the decrease in radius and that is dominant at low fluences (i.e., it is characterized by a large process cross-section), and another that tend to increase the radial etching rate and is dominant at high fluences (characterized by a small cross-section). We have tested this hypothesis by assuming that a simple two exponential law governs the fluence dependence of the pore diameter $D(\phi)$:

$$\frac{D(\phi)}{D(0)} = e^{-\sigma_1\phi} + A(1 - e^{-\sigma_2\phi}), \qquad (1)$$

where $D(0)$ is the diameter of the pores on the foils not irradiated with protons, σ_1 is the cross-section for the modifications introduced by the proton beam that cause a reduction in $D(\phi)$, σ_2 is the cross-section of modifications

introduced by the proton beam that causes an increase in $D(\phi)$, and A is the diameter ratio at very large fluences. There was no means to evaluate experimentally an accurate value of A, because of the fragility of the samples at large ϕ. On the other hand, the experimental curve suggests that $D(\phi)/D(0)$ is not far from unity in the useful fluence regime where the integrity of the foils is preserved. As for all fluences tested experimentally $D(\phi)/D(0) < 1$ (Fig. 2), we assumed for simplicity that at large fluences, $D(\phi)/D(0) \to 1$; i.e., $A = 1$ in (1). The result of a fit of (1) to the experimental data (including all 4 batches) is shown as a solid line in Fig. 2. The best fit was obtained for $\sigma_1 = (7.2 \pm 0.9) \times 10^{-14}$ cm^2 (or an effective modification radius R_1 of $\sim$1.5 nm) and $\sigma_2 = (5.7 \pm 0.4) \times 10^{-15}$ cm^2 (or an effective modification radius R_2 of $\sim$0.4 nm), assuming $A = 1$. The value of σ_1 changed only slightly as A is varied, but the effect of A in σ_2 is more significant. For example, if A is set to 1.5 (representing a 50% increase of the pore size at very large H^+ fluences), $\sigma_1 = (6.6 \pm 0.7) \times 10^{-14}$ cm^2 and $\sigma_2 = (3.3 \pm 0.2) \times 10^{-15}$ cm^2.

4 Discussion

Although it is clear that competitive processes induced by the proton beam at different rates or cross-sections alter the etching of the Au ion tracks, it is still necessary to identify what are the physicochemical mechanisms behind each process. The decrease in pore size due to the proton irradiation is consistent with a reduction in the radial or bulk etch rate v_B or an increase in the etching induction time. Negligible changes in the contact angle of proton irradiated foils in comparison with the virgin sample were detected (not more than 5% of the initial value of 86°), thus the changes in the etching response cannot be attributed to changes in the wetting properties of the foils, which could alter the induction time.

A reduced v_B could be caused by, e.g., crosslinking of the PC matrix induced by the proton beam. However, the GPC curves, shown in Fig. 3, indicate the predominance of chain scission in the irradiated samples at low fluences, a well known result for polycarbonate [15]. Thus, the changes in the molecular weight distribution caused by the proton beam cannot explain the initial decrease in v_B and the pore radius. On the contrary, chain scission could only be linked to the second process, the one that causes the growth of the pore size at larger fluences.

The decrease in the bulk etch rate and the pore radii may also be attributed to an *increase* in crystallinity caused by the proton irradiation, what would make the penetration and diffusion of the etchant slower. Figure 4 shows the X-ray diffraction measurements for the nonirradiated PC and samples bombarded by 18 MeV Au and subsequently
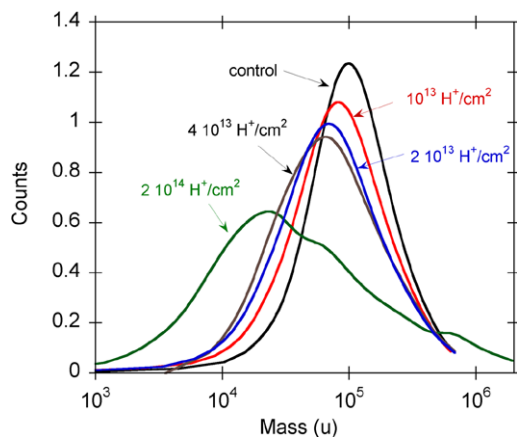
Fig. 3 (**a**) GPC curves for PC foils bombarded with 2 MeV H^+ + 18 MeV Au^{7+} at different H^+ fluences. The Au ion fluence was around 5×10^8 cm^{-2} for all samples. The control sample was only bombarded by the 18 MeV Au ions. GPC curves of foils irradiated in the reverse order (Au+H) (not shown) gave very similar results
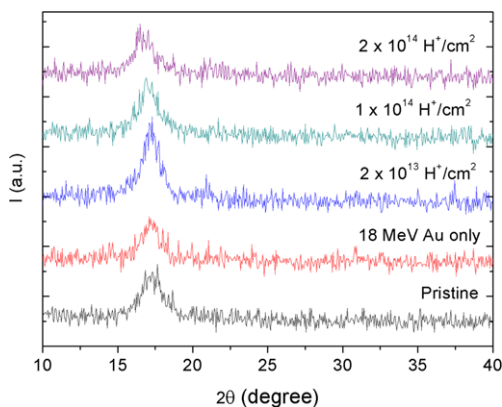

Fig. 4 X-ray diffraction patterns of the nonirradiated and irradiated PC foils. The foils were first irradiated with 18 MeV Au^{7+} at $\phi \sim 5 \times 10^8$ cm^{-2} and subsequently with 2 MeV H^+ at fluences indicated in the figure

with 2 MeV H^+. The area and width of the main diffraction peak at $2\theta = 17.2°$ was estimated from simple Gaussian fittings to the data, as in [16]. Figure 5 shows the area of the main diffraction peak as a function of proton fluence. This peak encompasses a 2θ range of $\sim 5°$, thus the uncertainty in the peak area introduced by the noise was estimated by measuring the area above the baseline, also in a 5° region located next to the peak, either from 10–15° or from 20–25°. These values are shown as error bars in Fig. 5.

The effect of the Au irradiation only was to reduce the crystallinity of the sample. The area of the main diffraction peak was reduced by $\sim 33\%$, even at fluences around 5×10^8 Au/cm^2 used for the production of the etched pores. Amorphization is the typical effect observed for heavy ion irradiation of PC [16, 17]. The H^+ irradiation, however, produced the opposite effect at low fluences. For a fluence of 2×10^{13} H^+/cm^2 the area of the 17.2° line became $\sim 30\%$
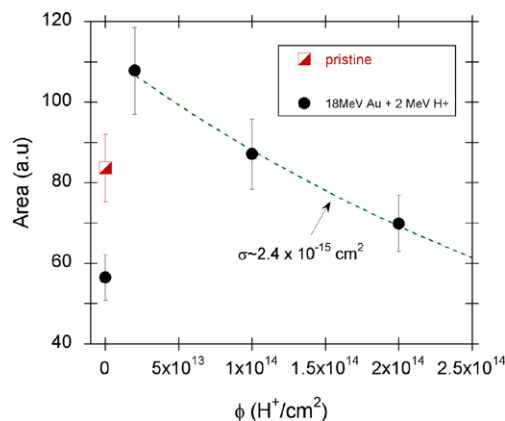

Fig. 5 Integral intensity of the main X-ray diffraction peak as a function of fluence for the pristine and irradiated samples. The *dashed line* is an exponential fit to the decaying part of the *curve*, starting at 2×10^{13} H^+/cm^2. The *error bars* are the areas due to noise, calculated in a region with a width similar to the peak extension ($2\theta = 5°$)

larger than the one for the pristine sample. The peak became also slightly narrower, indicating an increase in the average crystallite length, calculated using the Scherrer equation [18], from 4.0 ± 0.2 nm to 4.9 ± 0.2 nm. An increase in crystallinity in Makrofol-DE bombarded by 1 MeV H^+ at low fluences was also observed by Nouh et al. [19]. For larger proton fluences, amorphization is the dominant effect: the crystalline fraction slowly decreases with fluence (Fig. 5) and the main diffraction peak gets progressively broader.

It is interesting to note, that the shape of the curves of the diffraction peak area and of the pore radii as a function of fluence are correlated: both have a sharp variation at low fluences with a extreme close to $\phi = 2 \times 10^{13}$ cm^{-2}. Thus, the process of crystallinity enhancement induced by the proton beam evolves with a similar cross-section than that responsible for pore radius decrease (given by σ_1 extracted from Fig. 2). The set of data strongly indicates that the initial decrease in the pore radii is due to the increase in crystallinity induced by the proton irradiation.

The increase of the pore radii at large fluences is apparently a combination of the amorphization and chain scission (degradation) of the PC foils induced by the proton beam. The rate of amorphization, estimated from an exponential fit to the decaying part of the curve in Fig. 5, has a cross-section $\sigma_a \sim (2.4 \pm 0.2) \times 10^{-15}$ cm^2. The cross-section for chain scission was estimated from the curve of the fraction F of molecules in the vicinity of the most probable molecular weight ($\sim 10^5$ u) as a function of proton fluence. This fraction was extracted from the chromatograms by dividing the area of the curve in the molar mass region of $(0.9–1.1) \times 10^5$ u by the total area under the curve. The results are shown in Fig. 6. Fittings of the exponential curve $F = F_0 \exp(-\sigma_{cs}\phi)$ to the data in Fig. 6, yield $\sigma_{cs} = 5.3 \times 10^{-15}$ cm^2 for the (H+Au) case and 4.2×10^{-15} cm^2 for the (Au + H) sequence. It is seen that the cross-sections
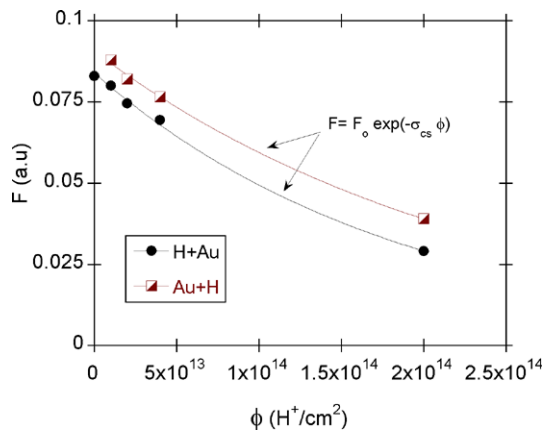
Fig. 6 Fraction F of molecules at the most probable molecular weight ($M_w = 10^5$ u) as a function of proton fluence for both irradiation orders, H + Au and Au + H. The fraction was calculated dividing the area of the GPC chromatograms between 0.9–1.1 $\times 10^5$ u by the total area under the curve. The solid lines are exponential fits to the data

for chain scission σ_{cs} and amorphization σ_a induced by the H$^+$ beam are comparable to σ_2 ($\sim 5.7 \times 10^{-15}$ cm^2) the cross-section that regulates the rate of regrowth of the pore radius with fluence.

The fact that the changes in the pore size are not sensitive to the irradiation order suggests that the structural alterations induced in the PC matrix by the proton beam are the determinant factors for the changes in the etching response. The perturbation of the defect distribution created along Au track by the proton beam seems to play a minor role.

5 Conclusion

The effect of light-ion irradiation on the pore size distribution of etched tracks produced by medium energy heavy ions (18 MeV Au) in polycarbonate was investigated. The perturbation introduced by the proton beam on the etching response of the foils caused initially a decrease in the mean etched pore size. The reduction effect was greatest at H$^+$ fluences around 2 to 5×10^{13} cm^{-2} and beyond that the pore radii started to grow again. This type of functional dependence with ϕ was observed irrespective of the order of the irradiation. This behavior was explained based on the action of two competitive effects produced by the H$^+$ irradiation with distinct cross-sections: one that causes the decrease in the pore diameter D and is dominant at low fluences and

another that tends to increase the radial etching rate (and D) and is dominant at high fluences. The initial decrease in the pore radii, with a characteristic cross-section close to 7×10^{-14} cm^2, is attributed to an increase in crystallinity. As the total irradiation builds up, this effect is surpassed by chain scission and amorphization of the polymer, leading to a gradual regrowth of the pore size at a lower rate with a cross-section $\sim 5 \times 10^{-15}$ cm^2. Light ion irradiation at low fluences may be used to simultaneously control the pore size and the mechanical properties of the etched foils.

References

1. R.L. Fleischer, P. Price, R.M. Walker, *Nuclear Tracks in Solids* (University of California Press, Berkeley, 1975)
2. R. Spohr, Ion Tracks, *Microtechnology* (Vieweg, Braunshweig, 1990)
3. P.Y. Apel, D. Fink, in D. Fink (ed.) *Transport Processes in Ion—Irradiated Polymers* (Springer, Berlin, 2004)
4. S.K. Chakarvarti, Radiat. Meas. **44**, 1085 (2008)
5. C. Milanez Silva, P. Varisco, A. Moehlecke, P.F.P. Fichtner, R.M. Papaléo, J. Eriksson, Nucl. Instrum. Methods Phys. Res. **206**, 486 (2003)
6. J. Jensen, A. Razpet, M. Skupinski, G. Possnert, Nucl. Instrum. Methods Phys. Res. **246**, 119 (2006)
7. R.G. Musket, J.M. Yoshiyama, R.J. Contolini, J.D. Porter, J. Appl. Phys. **91**, 5760 (2002)
8. M. Toulemonde, C. Trautmann, E. Balanzat, K. Hjort, A. Weidinger, Nucl. Instrum. Methods Phys. Res. **216**, 1 (2004)
9. G. Guillot, F. Rondelez, J. Appl. Phys. **52**, 7155 (1981)
10. T.W. Cornelius, P.Y. Apel, B. Schiedt, C. Trautmann, M.E. Toimil-Molares, S. Karim, R. Neumann, Nucl. Instrum. Methods Phys. Res. **265**, 553 (2007)
11. N. Sertova, E. Balanzat, M. Toulemonde, C. Trautmann, Nucl. Instrum. Methods Phys. Res. **267**, 1039 (2009)
12. S.P. Tripathy, R. Mishra, K.K. Dwivedi, D.T. Khathing, S. Ghosh, D. Fink, Radiat. Meas. **36**, 107 (2003)
13. H. Hanot, E. Ferain, Nucl. Instrum. Methods Phys. Res. **267**, 1019 (2009)
14. See SRIM 2010 homepage by J. Ziegler. http://www.srim.org/SRIM/SRIMINTRO.htm
15. A. Torikai, T. Murata, K. Fueki, Polym. Degrad. Stab. **7**, 55 (1984)
16. Y. Sun, Z. Zhu, Z. Wang, Y. Jin, J. Liu, M. Hou, Q. Zhang, Nucl. Instrum. Methods Phys. Res. **209**, 188 (2003)
17. L. Singh, K. Samra, Nucl. Instrum. Methods Phys. Res. **263**, 458 (2007)
18. A. Patterson, Phys. Rev. **56**, 978 (1939)
19. S.A. Nouh, A.A. Naby, P.J. Sellin, Radiat. Meas. **42**, 1655 (2007)